

Features of the $\pi^+d \rightarrow \pi^+\pi^+\pi^-d$ reaction at 6 GeV/c

J. Diaz,* F. A. DiBianca,[†] W. J. Fickinger, J. A. Malko, and D. K. Robinson
Case Western Reserve University, Cleveland, Ohio 44106[‡]

S. Dado, A. Engler, G. Keyes, and R. W. Kraemer
Carnegie-Mellon University, Pittsburgh, Pennsylvania 15213[§]

(Received 29 January 1975)

We have studied the coherent $\pi^+d \rightarrow \pi^+\pi^+\pi^-d$ reaction using a sample of 4019 events having a visible final-state deuteron. The total cross section, corrected for invisible deuteron events, was found to be $380 \pm 50 \mu\text{b}$. The main features of the data are the large production of ρ^0 (90%), with a corresponding $\rho^0\pi^+$ enhancement in the A_1 region, and the observation of the $d\pi$ enhancement at ~ 2.2 GeV.

I. INTRODUCTION

A number of groups have reported analyses of the coherent reaction

$$\pi^+d \rightarrow \pi^+\pi^+\pi^-d \quad (1)$$

for incident momenta between 4.2 and 13 GeV/c.¹⁻¹⁰ The main features of the reaction in the 5 to 7 GeV/c region are the large production of ρ^0 , with a corresponding $\rho\pi$ enhancement in the A_1 region, and the observation of the $d\pi$ enhancement at ~ 2.2 GeV (the d^*). We present results from our analysis of reaction (1) at 6 GeV/c incident momentum. The data come from a 930 000-picture exposure of the deuterium-filled Argonne National Laboratory 30-in. bubble chamber. The present analysis is based on a sample of 4019 events which fit reaction (1), where the deuteron was required to be visible and stopping.¹¹

II. MOMENTUM TRANSFER DISTRIBUTION AND CROSS SECTION

As expected for a coherent channel, the reaction exhibits a large diffraction peak. Figure 1 shows the distribution of $t' \equiv |t_{dd} - t_{\min}|$ for the 4019 events, where t_{dd} is the square of the four-momentum transfer between the initial and final deuterons. The strong falloff in this distribution at small momentum transfer is due to losses from invisible deuteron recoils. The shaded area represents corrections for scanning losses due to steeply dipping deuteron recoils, applied in the region¹² $t' > 0.03$ (GeV/c)². These corrections were deduced from a study of the azimuthal distributions of the recoiling deuteron about the beam direction. A fit to the distribution in Fig. 1 of the form $ae^{bt'}$ yields a slope parameter $b = (31.3 \pm 0.9)$ (GeV/c)⁻² ($\chi^2/\text{ND} = 4.5/11$) in the range $0.03 \leq t' < 0.16$ (GeV/c)². Figure 2 shows a plot of the slope parameter b as a function of the 3π effective mass ($M_{3\pi}$). The variation of b seen in Fig. 2 can be compared to the essentially constant slope found for

this same reaction at 11.7 GeV/c incident momentum.¹⁰ The change in the $M_{3\pi}$ dependence of b with increasing incident momentum may be indicative of effects due to a lower lying Regge trajectory, since f exchange is expected to contribute to this reaction in addition to the dominant Pomeron-exchange terms.

To calculate the cross section we correct for the unseen deuteron events by extrapolating the fit in Fig. 1 to $t'=0$. We obtain in this way a total $\pi^+d \rightarrow \pi^+\pi^+\pi^-d$ cross section of $380 \pm 50 \mu\text{b}$. A comparison of this cross section with the values found for the same reaction at 8 GeV/c ($340 \pm 40 \mu\text{b}$)

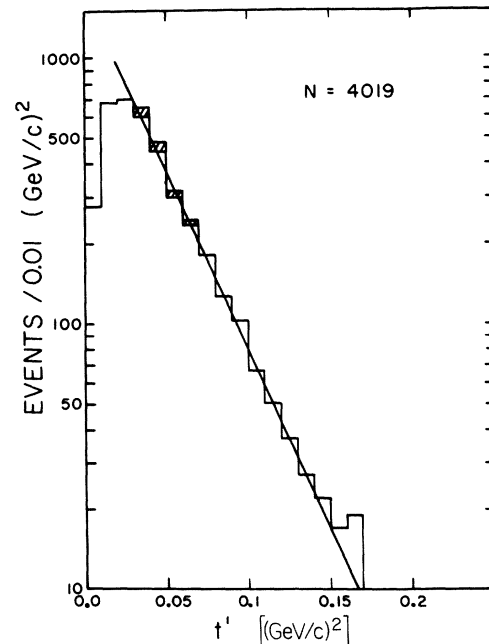


FIG. 1. Histogram of $t' \equiv |t_{dd} - t_{\min}|$, where t_{dd} is the square of the four-momentum transfer between the initial and final deuterons. The straight line is a fit to the exponential form $e^{(-31.3 \pm 0.9)t'}$. To convert this histogram to $d\sigma/dt'$ use (14.5 ± 1.9) events/ μb .

(see Ref. 9) and 11.7 GeV/c ($370 \pm 60 \mu\text{b}$) (see Ref. 10) shows that already at 6 GeV/c the $\pi d \rightarrow \pi\pi\pi d$ cross section has leveled off.

III. RESONANCE PRODUCTION AND THE d^* ENHANCEMENT

Figure 3(a) shows the $\pi^+\pi^-$ effective mass distribution (two combinations per event) for the total sample. There is a prominent ρ^0 signal plus a shoulder in the f^0 region. The f^0 signal is seen more clearly in Fig. 3(b) which shows the $\pi^+\pi^-$ mass distribution for events in the A_3 region (defined by $1.5 \leq M_{3\pi} < 1.8$ GeV). The smooth curve in Fig. 3(a) is the result of a fit to two Breit-Wigner terms plus a polynomially modified peripheral phase-space background.¹³ In this fit the mass and width of the f^0 were fixed at $M = 1.27$ GeV, $\Gamma = 0.163$ GeV.¹⁴ The fit ($\chi^2/\text{ND} = 38/30$) yields $(90 \pm 3)\%$ ρ^0 , $(5 \pm 1)\%$ f^0 , $M_\rho = 0.769 \pm 0.003$ GeV, $\Gamma_\rho = 0.147 \pm 0.009$ GeV.

The unshaded histogram in Fig. 4(a) shows the $d\pi^+$ effective mass distribution (two combinations per event) where the well-known d^* enhancement at ~ 2.2 GeV is strongly evident. The d^* enhancement has been seen by many investigators and has been successfully explained as a final-state interaction between an exchanged virtual pion and one of the bound nucleons in the deuteron.¹⁵ Its effective mass distribution shows an approximate Breit-Wigner shape. The solid curve in Fig. 4(a) is a fit to the data of a smooth background plus a Breit-Wigner term. This fit yields $(26 \pm 2)\%$ d^{*++} , $M_{d^{*++}} = 2.16 \pm 0.01$ GeV, $\Gamma_{d^{*++}} = 0.19 \pm 0.02$ GeV. This mass and width are compatible with previous parameterizations of the d^* in this and other channels.¹⁶ Figure 4(b) shows the $d\pi^-$ effective mass distribution for the total sample (unshaded histogram) and for the sample obtained after we removed events in the ρ^0 region (shaded). Counting the

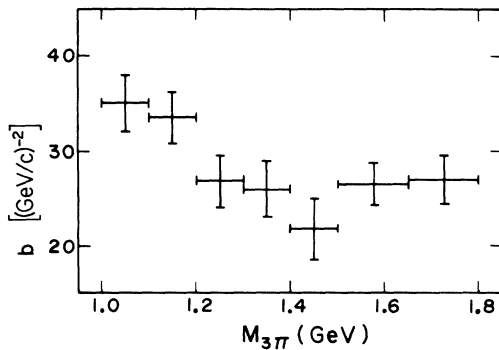


FIG. 2. The slope parameter b obtained by fitting the dN/dt' distribution to the form $ae^{-bt'}$ for various $M_{3\pi}$ intervals.

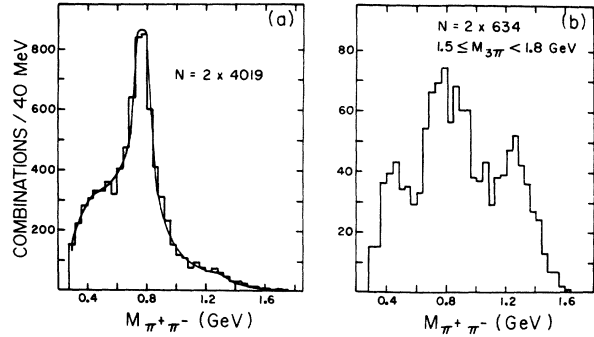


FIG. 3. (a) Histogram of the $\pi^+\pi^-$ mass distribution for the total sample of events. The smooth curve is a fit to the data of two Breit-Wigner terms plus a smooth background. (b) Histogram of the $\pi^+\pi^-$ mass distribution for events with $1.5 \leq M_{3\pi} < 1.8$ GeV.

events above a smooth background (solid curve) for the ρ^0 -subtracted distribution and correcting for the ρ^0 cut we estimate that there is less than $\sim 4\%$ d^{*0} in reaction (1).

It has been suggested by Deery *et al.*³ that the d^* enhancement seen in their $\pi^+d \rightarrow \pi^+\pi^+\pi^-d$ data at 5.4 GeV/c can be described as resulting from the kinematics of the $\rho d\pi$ final state. To investigate the possibility of a kinematic interpretation for the d^* in our data we have used the Monte Carlo method to generate $\pi d \rightarrow \rho d\pi$ ($\rho \rightarrow 2\pi$) events, where the

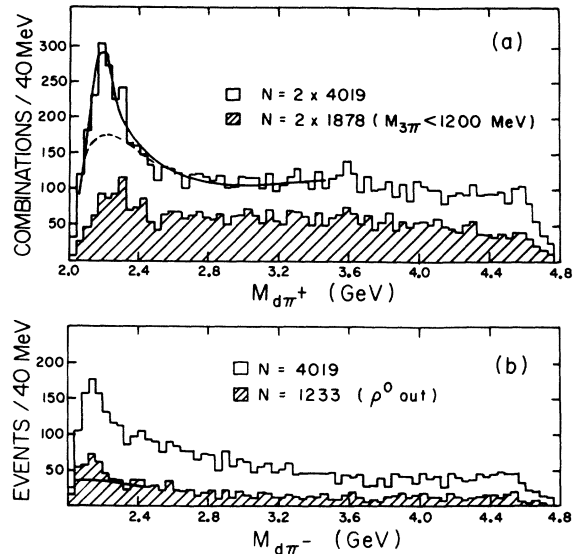


FIG. 4. (a) Histogram of the $d\pi^+$ effective-mass distribution for the total sample (unshaded) and for events with $M_{3\pi} < 1.2$ GeV (shaded). (b) Histogram of the $d\pi^-$ effective-mass distribution for the total sample (unshaded). The shaded histogram in (b) was obtained by removing events for which $0.64 < M_{\pi^+\pi^-} < 0.84$ GeV. The curves are described in the text.

events were generated so as to reproduce the experimentally observed t_{dd} distribution.¹⁷ The dashed curve in Fig. 4(a) shows the Monte Carlo prediction in the region of the d^* , normalized to 2×4019 combinations, and is seen to give a poor description of the enhancement.

Recently an enhancement in the $d\pi^+\pi^-$ system was seen in the $\pi^-d \rightarrow \pi^-\pi^-\pi^+d$ channel at 15 GeV/c for peripheral $d\pi^+\pi^-$ combinations after removing events associated with the ρ , f , g , and A_1 enhancement also seen in this channel¹⁸. As reported in Ref. 18 the enhancement is well described by a model having a dominant contribution from Pomeron exchange. This being the case, one might not expect an appreciable reduction in its production cross section in going from 15 to 6 GeV/c incident momentum. Figure 5 shows the effective mass distribution for peripherally produced $d\pi^+\pi^-$ combinations in our data, where we have removed contributions from ρ , f , and A_1 with cuts similar to those of Ref. 18. Approximately 80% of the events are contained in the region $M_{d2\pi} < 3.0$ GeV. The distribution in Fig. 5 is in reasonable agreement with the data of Ref. 18. We note, however, that our data do not contain the invisible deuteron recoil events which should be important at low $d2\pi$ masses.

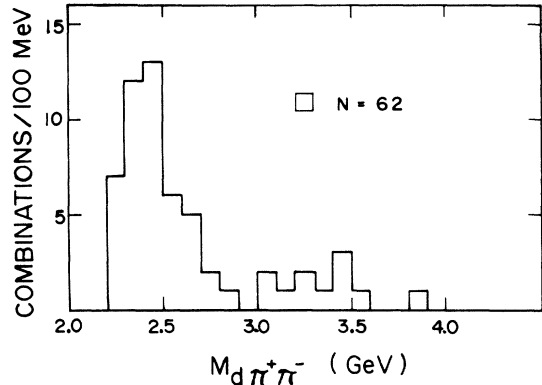


FIG. 5. The effective-mass distribution for $d\pi^+\pi^-$ combinations having $t'_{d\pi^+\pi^-} < 0.08$ (GeV/c)² and $M_{3\pi} < 1.6$ GeV. In addition, we exclude all events which have a $\pi^+\pi^-$ combination in the ρ region ($0.64 < M_{\pi^+\pi^-} < 0.84$ GeV) or f^0 region ($1.2 < M_{\pi^+\pi^-} < 1.34$ GeV).

IV. THREE-PION SYSTEM

Figure 6(a) (unshaded histogram) shows the 3π effective mass distribution in which we see a broad enhancement in the A_1 region and a small accumu-

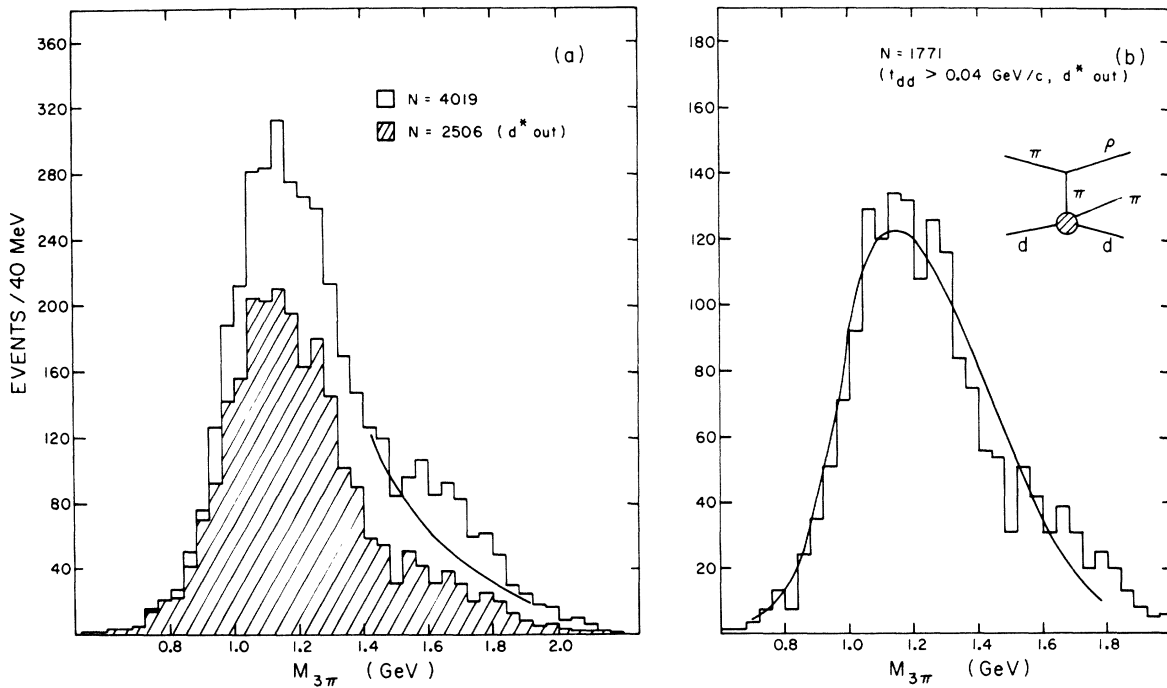


FIG. 6. (a) The 3π effective-mass distribution for all events (unshaded) and the events having $M_{d\pi^+} > 2.32$ GeV (shaded). (b) The 3π effective-mass distribution for events with $|t_{dd}| > 0.04$ (GeV/c)² and $M_{d\pi^+} > 2.32$ GeV. The solid curve is described in the text.

lation of events in the A_3 region. There are no narrow resonances evident in this figure. The A_1 enhancement is essentially all $\rho\pi$; a fit to the $\pi^+\pi^-$ effective mass distribution for events having $0.96 \leq M_{3\pi} < 1.24$ GeV is consistent with 100% ρ^0 production. There are ~ 180 events above a smooth hand-drawn background (solid curve) in the A_3 region ($1.5 \leq M_{3\pi} < 1.8$ GeV); this number is consistent with the $\sim 5\%$ f^0 found in the fit to the 2π mass distribution in Fig. 3(a).

The d^{**} enhancement mentioned in the previous section is found to affect predominantly the high-mass region of the 3π system. The shaded distribution in Fig. 6(a) is the 3π mass plot with d^* events removed. The shaded distribution in Fig. 4(a) shows the $d\pi^+$ effective mass distribution for events having $M_{3\pi} < 1.2$ GeV, and shows only a very weak signal for d^{**} .

It has been shown previously that one can describe the A_1 $\rho\pi$ enhancement without the need for a resonance interpretation.⁹ To describe the $\rho\pi$ mass distribution we have used the model due to Berger¹⁹, in which we assume Reggeized π exchange and ignore the small f^0 and nonresonant final states [see diagram inserted in Fig. 6(b)]. Outside the d^* region the contribution from the πd vertex may be approximated by the on-shell elastic-scattering amplitude having the form $[s_1 - (M_\pi + M_d)^2] [s_1 - (M_\pi - M_d)^2] e^{-A t_{dd}}$ where $s_1 = M_{d\pi}^2$ and A is adjusted to fit the experimental t_{dd} distribution.¹⁹ Because of scanning losses at low t_{dd} values, we apply the model only to events having $t_{dd} \geq 0.04$ GeV/c². Figure 6(b) shows the $M_{3\pi}$ distribution for the non- d^* events ($M_{d\pi} \geq 2.32$ GeV) with $t_{dd} \geq 0.04$ GeV/c². The solid curve is the prediction of the model (corrected for the t_{dd} and d^* cuts) normalized to the total number of events, and is seen to be in reasonable agreement with the data in the A_1 region.²⁰

We have performed an analysis of the spin content of the 3π system, using the normalized moments $\langle P_l \rangle$ of $P_l(\cos\theta)$.²¹ Here P_l is the l th Legendre polynomial and θ is the polar angle of the normal to the 3π plane in the Gottfried-Jackson frame of the 3π system. Figure 7 shows the variation of these moments as a function of the 3π mass, for $l=2, 4, 6, 8$. (The odd moments vanish because of the symmetry of the $\cos\theta$ distribution about $\cos\theta=0$). For a diffractively produced 3π system the spin parity should be in the series $0^-, 1^+, 2^-, \dots$. We see that $\langle P_2 \rangle$ is nonzero over the entire 3π mass range while all the higher moments are essentially zero in the A_1 region ($1.0 \leq M_{3\pi} < 1.3$ GeV).²² These results are consistent with the previously established spin $J^P=1^+$ for the A_1 enhancement.¹⁴ We note that $\langle P_4 \rangle$ is essentially zero for low 3_π mass and becomes non-

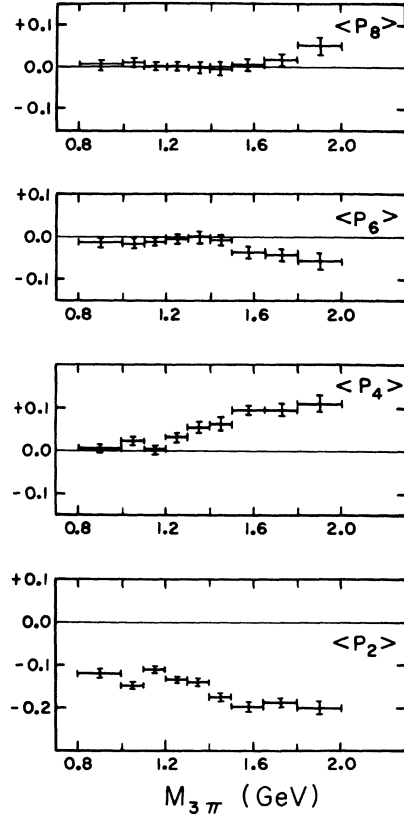


FIG. 7. The normalized moments of the Legendre polynomial $P_l(\cos\theta)$, as a function of the 3π effective mass. Here θ is the polar angle of the normal to the 3π plane in the Jackson frame of the 3π system.

zero in the A_2 mass region; both $\langle P_4 \rangle$ and $\langle P_6 \rangle$ are significantly nonzero in the high-mass region ($M_{3\pi} > 1.5$ GeV). There are indications of an A_2 signal in the d^* -removed 3π mass plot [shaded histogram Fig. 6(a)]. We find an excess of 120 events above a smooth hand-drawn background in

TABLE I. The ρ_{00} , $\rho_{1,-1}$, and $\text{Re}\rho_{10}$ matrix elements (assuming $J^P=1^+$) for the 3π system in the mass region $0.96 \leq M_{3\pi} < 1.2$ GeV. The matrix elements are calculated for two t_{dd} regions in both the Gottfried-Jackson and the helicity frames.

| $0.0 \leq t_{dd} < 0.05$ (GeV/c) ² | | $0.05 \leq t_{dd} < 0.15$ (GeV/c) ² | |
|---|--|--|--|
| Gottfried-Jackson frame | | | |
| $\rho_{00} = 1.04 \pm 0.03$ | | $\rho_{00} = 1.00 \pm 0.04$ | |
| $\rho_{1,-1} = -0.14 \pm 0.05$ | | $\rho_{1,-1} = -0.16 \pm 0.06$ | |
| $\text{Re}\rho_{10} = 0.04 \pm 0.02$ | | $\text{Re}\rho_{10} = -0.07 \pm 0.03$ | |
| Helicity frame | | | |
| $\rho_{00} = 0.93 \pm 0.04$ | | $\rho_{00} = 0.89 \pm 0.04$ | |
| $\rho_{1,-1} = -0.20 \pm 0.05$ | | $\rho_{1,-1} = -0.12 \pm 0.05$ | |
| $\text{Re}\rho_{10} = 0.21 \pm 0.02$ | | $\text{Re}\rho_{10} = 0.22 \pm 0.03$ | |

the 1.2–1.4 GeV region, corresponding to an upper limit of 20 μb for A_2^+ production.

It has been suggested that diffractive processes may exhibit either s - or t -channel helicity conservation.²³ To investigate this point we have used the method of moments to calculate the matrix elements ρ_{00} , $\rho_{1,-1}$, and $\text{Re } \rho_{10}$ for a 1^+ spin assignment for the 3π system.²⁴ Table I shows the results for two t_{dd} intervals for events in the A_1 region ($0.96 \leq M_{3\pi} < 1.24$ GeV). The matrix elements were calculated in both the Gottfried-Jackson and helicity frames. For s -channel (t -channel) helicity conservation we would expect $\rho_{00} = 1$ and

all other elements to be zero in the helicity (Gottfried-Jackson) frame. The data in Table I are seen to favor t -channel helicity conservation. This result is similar to the observation of t -channel helicity conservation for diffractively produced A_1 in the reactions $\pi^+p \rightarrow A_1^+p \rightarrow \pi^+\pi^+\pi^-p$ at 8 and 16 GeV/c.²⁵

We thank the staffs of the ZGS and the 30-in. ANL bubble chamber as well as our two scanning groups. We also thank Dr. J. F. Owens for useful discussions.

*Presently at Junta de Energia Nuclear, Madrid, Spain.

†Presently at Fermi National Accelerator Laboratory, Batavia, Illinois.

‡Work supported by the National Science Foundation.

§Work supported in part by the U. S. Atomic Energy Commission.

¹G. Vegni, H. Winzeler, P. Zaniol, P. Fleury, and G. DeRosny, *Phys. Lett.* **19**, 526 (1965) (at 6 GeV/c).

²A. M. Cnops, P. V. C. Hough, F. R. Huson, I. R. Kenyon, J. M. Scarr, I. O. Skillicorn, H. O. Cohn, R. D. McCulloch, W. M. Bugg, G. T. Condo, and M. M. Nussbaum, *Phys. Lett.* **29B**, 45 (1969) (8 GeV/c).

³B. J. Deery, N. N. Biswas, N. M. Cason, T. H. Groves, P. B. Johnson, V. P. Kenney, J. A. Poirier, O. A. Sander, P. H. Smith, and W. D. Shephard, *Phys. Rev. D* **3**, 635 (1971) (5.4 GeV/c).

⁴D. Harrison, J. D. Prentice, E. C. West, T. S. Yoon, J. T. Carroll, M. W. Firebaugh, and W. D. Walker, *Phys. Rev. D* **5**, 2730 (1972) (6.95 GeV/c).

⁵B. Eisenstein and H. Gordon, *Phys. Rev. D* **1**, 841 (1970) (4.2 GeV/c).

⁶R. Vanderhaghen, G. DeRosny, N. Armenise, B. Ghidini, A. Romano, A. Forino, and M. Goldberg, *Nucl. Phys.* **B13**, 329 (1969) (5 GeV/c).

⁷A. Forino, R. Gessaroli, L. Lendinara, G. Quareni, A. Quareni-Vignudelli, N. Armenise, B. Ghidini, V. Picciarelli, A. Romano, A. Cartacci, M. G. Daghiana, M. Della Corte, G. Dicaporiaco, J. Laberrigue-Frolow, Nguyen Huu Khanh, J. Quinquart, M. Sene, W. Fickinger, and O. Goussu, *Phys. Lett.* **19**, 68 (1965) (4.5 GeV/c).

⁸K. Paler, R. C. Badewitz, H. R. Barton, Jr., D. H. Miller, T. R. Palfrey, Jr., and J. Tebes, *Phys. Rev. Lett.* **26**, 1675 (1971) (13 GeV/c).

⁹A. M. Cnops, P. V. C. Hough, F. R. Huson, I. R. Kenyon, J. M. Scarr, I. O. Skillicorn, H. O. Cohn, R. D. McCulloch, W. M. Bugg, G. T. Condo, and M. M. Nussbaum, *Phys. Rev. Lett.* **21**, 1609 (1968).

¹⁰D. Kemp, M. C. Scarrot, R. Contri, D. Teodoro, G. Tomasini, E. Calligarich, S. Ratti, J. Huc, G. DeRosny, R. Sosnowski, M. Barrier, G. Bozoki, A. Brandao, and Nguyen Huu Khanh, report submitted to the Seventeenth International Conference on High Energy Physics, London, 1974 (unpublished).

¹¹Approximately 80% of the fits to reaction (1) were am-

biguous with the fit to the broken deuteron channel $\pi^+d \rightarrow p_s n \pi^+ \pi^+ \pi^-$, where p_s is a spectator proton. A study of the $\cos\theta_{p_s, n}$ and $M_{p_s, n}^2$ distributions for the broken deuteron fits showed that these ambiguous events were essentially all $\pi d \rightarrow \pi \pi d$ events. We estimate that the contamination from broken-deuteron events in our sample is less than 2%.

¹²Below $t' = 0.03$ (GeV/c)² the losses from events which do not leave a visible deuteron recoil in the chamber are more important than scanning losses due to steeply dipping tracks.

¹³The effective mass distribution was fitted to the form $dN/dM_{2\pi} = (\alpha P + \beta_1 F_{BW1} + \beta_2 F_{BW2}) F_{PS}$, where α , β_1 , and β_2 are constants representing the amount of background ρ^0 and f^0 , respectively, P is a polynomial quadratic in $M_{2\pi}$, F_{BW1} are simple Breit-Wigner terms for the ρ and f of the form $1/[(M_{2\pi} - M_{RES})^2 + (\Gamma_{RES}/2)^2]$, and F_{PS} is a Monte Carlo generated peripheral phase-space factor generated to reproduce the experimental t_{dd} distribution.

¹⁴Particle Data Group, *Phys. Lett.* **50B**, 1 (1974).

¹⁵See for example Ref. 16 and A. Fridman, Centre de Recherches Nucléaires de Strasbourg Report No. CNR/HE 74-4 (unpublished), p. 71.

¹⁶H. Braun, D. Evrard, A. Fridman, J. P. Gerber, G. Maurer, A. Michalon, B. Schiby, R. Strub, and C. Voltolini, *Phys. Rev. D* **2**, 1212 (1970).

¹⁷For simplicity we assume 100% ρ production. The Monte Carlo events are generated so as to reproduce the experimentally observed mass, width, and asymmetric decay of the ρ seen in the data.

¹⁸H. H. Bingham, W. B. Fretter, W. R. Graves, F. C. Porter, L. Stutte, G. P. Yost, L. A. Dunn, R. Harris, H. J. Lubatti, K. Moriyasu, and W. J. Podolsky, *Nucl. Phys.* **B88**, 275 (1975).

¹⁹Edmond L. Berger, *Phys. Rev.* **166**, 1525 (1968).

²⁰We use a Monte Carlo method to calculate the model prediction. To allow for the width of the ρ the dipion mass for each event is chosen from a Breit-Wigner distribution with $M = 0.769$ GeV, $\Gamma = 0.147$ GeV.

²¹A more detailed partial-wave analysis of the 3π system is in progress, using a method similar to that of D. V. Brockway, Ph.D. thesis, 1970, University of Illinois, Urbana (unpublished).

²²These results are not significantly changed by remov-

ing events in the d^{**} region.

²³See, for example, Aachen-Berlin-Bonn-CERN-Cracow-Heidelberg-London-Vienna-Warsaw Collaboration (J. V. Beaupr e *et al.*, Phys. B47, 51 (1972).

²⁴Following S. M. Berman and M. Jacob [Phys. Rev. 139, B1023 (1965)] we write the decay angular distribution in terms of the polar angle (θ) and azimuthal angle (ϕ) of the normal to the 3π decay plane in the 3π rest sys-

tem. The matrix elements are then given by $\rho_{00} = 2 - 5 \langle \cos^2\theta \rangle$, $\rho_{1,-1} = \frac{5}{2} \langle \sin^2\theta \cos 2\phi \rangle$, and $\text{Re}\rho_{10} = (5/\sqrt{2}) \langle \sin\theta \cos\theta \cos\phi \rangle$ in either the Gottfried-Jackson or helicity frame.

²⁵Aachen-Berlin-Bonn-CERN-Cracow-Heidelberg-London-Vienna Collaboration (J. V. Beaupr e *et al.*), Phys. Lett. 34B, 160 (1970).